Computers and Concrete, *Vol. 29, No. 5 (2022) 335-346*
https://doi.org/10.12989/cac.2022.29.5.335

Durability properties of fly ash-based geopolymer mortars with different quarry waste fillers

Yosra Tammam*[1], Mucteba Uysal[2a] and Orhan Canpolat[2b]

[1]*Civil Engineering Department, Istanbul Gelisim University, Istanbul, Turkey*
[2]*Civil Engineering Department, Faculty of Civil Engineering, Yildiz Technical University, Davutpasa Campus, Istanbul, Turkey*

(*Received August 4, 2021, Revised April 5, 2022, Accepted May 2, 2022*)

Abstract. Geopolymers are an important alternative material supporting recycling, sustainability, and waste management. Durability properties are among the most critical parameters to be investigated; in this study, the durability of manufactured geopolymer samples under the attack of 10% magnesium sulfate and 10% sodium sulfate solution was investigated. 180 cycles of freezing and thawing were also tested. The experimentally obtained results investigate the durability of geopolymer mortar prepared with fly ash (class F) and alkali activator. Three different quarry dust wastes replaced the river sand aggregate: limestone, marble, and basalt powder as fine filler aggregate in three different replacement ratios of 25%, 50%, and 75% to produce ten series of geopolymer composites. The geopolymer samples' visual appearance, weight changes, UPV, and strength properties were studied for up to 12 months at different time intervals of exposure to sulfate solutions to investigate sulfate resistance. In addition, Scanning Electron Microscopy (SEM), EDS, and XRD were used to study the microstructure of the samples. It was beneficial to include quarry waste as a filler aggregate in durability and mechanical properties. The compact matrix was demonstrated by microstructural analysis of the manufactured specimens. The geopolymer mortars immersed in sodium sulfate showed less strength reduction and deterioration than magnesium sulfate, indicating that magnesium sulfate is more aggressive than sodium sulfate. Therefore, it is concluded that using waste dust interrogation with partial replacement of river sand with fly ash-based geopolymers has satisfactory results in terms of durability properties of freeze-thaw and sulfate resistance.

Keywords: durability; fly ash; freezing-thawing; geopolymer; microstructure; quarry waste materials; sulfate environment

1. Introduction

In 2010, the production of ordinary Portland cement (OPC), the predominant binder used in construction, was about 3.27 billion m/t and will increase to 4.83 billion m/t by 2030, which means that CO_2 emissions from cement production worldwide will also increase by about 7% (Madlool *et al.* 2011, Pacheco-Torgal *et al.* 2012, Ziada *et al.* 2022a). Researchers have begun to focus on waste materials known as geopolymer mortars to transform sustainable cementitious materials. These materials, such as fly ash, slag, and metakaolin, have a high aluminosilicate content. They are activated with an alkali activator to bind the aggregates by forming C-S-H or C-A-S-H and N-A-S-H to produce the geopolymer concrete (Brough and Atkinson 2002, Douglas *et al.* 1991, Fernández-Jiménez *et al.* 1999 Neupane *et al.* 2018, Puertas and Fernández-Jiménez 2003).

In addition to achieving high strength properties, fly ash conserves nature to produce environmentally friendly composites (Ziada *et al.* 2022b). The activation of aluminum silicate forms a stable C-S-H gels matrix by activating fly ash and slag-based geopolymer gel and improving the strength properties (Bernal *et al.* 2011, 2012). Furthermore, the increase or decrease in compressive strength' of geopolymer concrete depends on the Si/Al ratio and the type of binder used (P Duxson *et al.* 2007, Peter Duxson *et al.* 2005, He *et al.* 2016, Wongpa *et al.* 2010). Curing a geopolymer mixture (alumina-silica) can be carried out at ambient temperature or oven curing (Bonen and Cohen 1992). According to (Škvára *et al.* 2005), the resistance of geopolymer concrete under acid and sulfate attack action is high due to its excellent binding, high compressive strength, high density, and low drying shrinkage. Carbonation and sulfate attack effects that cause corrosion are among the main factors that reduce the durability of the geopolymer structure (Džunuzović *et al.* 2017, Valencia Saavedra *et al.* 2016). Previous studies performed that the durability performance of geopolymer concrete is severely degraded when exposed to sulfate attack for a long time (Abora *et al.* 2014, Chotetanorm *et al.* 2013, Singh *et al.* 2015, Sukmak *et al.* 2015). Researchers emphasized that it is important to investigate methods and materials that reduce the effect of sulfate to increase the durability of geopolymers. Under sulfate exposure, the OPC shows deterioration related to gypsum and ettringite formation, causing expansion and cracking of the specimen. The destruction of C-S-H causes the decay under sulfate attack. According to the experimental results of (Bakharev 2005), the strength of geopolymers based on fly ash

*Corresponding author, Ph.D.
E-mail: ymtammam@gelisim.edu.tr

ISSN: 1598-8198 (Print), 1598-818X (Online)

improves after 150 days under the attack of sodium and magnesium sulfate (5%) due to the diffusion of Mg and Ca on the surface of the geopolymer sample. Previous studies for (Sagoe-Crentsil *et al.* 2013, Scrivener and Young 1997) founds that the geopolymer concretes show marginal changes after 360 days of sulfate exposure, which means that the durability depends on the type of activation materials used. In the studies of (Škvára *et al.* 2005), no dimensional changes were observed after 720 days of sulfate exposure, neither the formation of expansive phases nor the increase of strength properties. Using sodium silicate and sodium hydroxide as activators of fly ash geopolymer concrete, Puertas *et al.* found that the specimens showed excellent resistance to the attack of sulfate solutions. Moreover, the specimens activated only with sodium hydroxide showed little degradation by gypsum and ettringite (Puertas *et al.* 2002). Ismail *et al.* (2013) investigated the behavior of alkali silicate activated fly ash/slag geopolymer binders exposed to various types of sulfate exposure for three months, primarily by immersion in 5 percent magnesium sulfate or 5 percent sodium sulfate solutions. Immersion in $MgSO_4$ solution results in extensive physical degradation of the pastes, but not in Na_2SO_4 solution. Calcium sulfate dihydrate (gypsum) forms in pastes immersed in $MgSO_4$, the expansive effect of which is known to be particularly detrimental to the substrate but is not observed under Na_2SO_4 conditions. Earlier investigations showed that pozzolan addition to ordinary cement mortars increased the mortar resistance to Na_2SO_4 (Aye and Oguchi 2011). In study of (Zhang *et al.* 2017), geopolymers with low calcium content were better resistant to $MgSO_4$ sulfate. In general, different types of geopolymer mortars had better magnesium sulfate resistance than OPC mortars (Elyamany *et al.* 2018).

However, a limited number of studies are concerned with the freeze-thaw cycle on geopolymer concrete. Cai *et al.* (2013) tested the freeze-thaw effect on a slag geopolymer matrix and found that the specimens exhibited high durability, and the coefficient of durability was about 90%. Temuujin *et al.* (2014) concluded that the geopolymer concrete made from fly ash shows damage after applying 40 freeze-thaw cycles. Slavik *et al.* (2008) found that after performing 50 freeze-thaw cycles, the compressive strength of specimens with low calcium content was 20% lower. It was proved that alkali-activated slag geopolymer showed good performance in freeze-thaw resistance. Krivenko (1999) studied the effect of different types of alkaline activator solutions on freeze-thaw resistance. It was found that the geopolymer slag concrete activated with sodium silicate showed good performance in freeze-thaw resistance due to its less porous structure. According to (Fu *et al.* 2011), activated slag concrete can withstand at least 300 freeze-thaw cycles. Joseph and Mathew (2012) experimented with geopolymer concretes made from fly ash and investigated the effect of filler content. Different filler quantities and other features such as curing and the effect of a chemical activator on matrix properties were investigated. The results showed that after ensuring other optimum factors, the proper ratio of filler content could determine the appropriate mix ratio in geopolymer concrete. The concrete prepared in this way has good physical, microstructural and durability properties.

Quarry dust accounts for 15% of aggregate production (Hill *et al.* 2001). During cutting and polishing, nearly 25% of stones used in constructions turn into waste stone sludge (Chang *et al.* 2010). Environmental severe problems emerge when stone waste is stored and disposed of without treatment or recycling. Also, Galetakis and Raka (2004) found that 10-15% dust to replace cement and limestone powder improved the strength properties. Another research by (Celik and Marar 1996) replaced sand up to 30% and kept all other parameters constant. It showed that using dust stone up to 10% instead of sand improved the strength properties of concrete. Moreover, it was reported that the strength properties of concrete were improved when waste dust stone was used for up to 40% (Sahu *et al.* 2003). Also, after using dust rock in a certain ratio, the mechanical properties decreased (Kapgate and Satone 2013). Substitution of coarse aggregate with waste dust aggregate up to 10% had no adverse effect as far as corrosion is concerned (Maslehuddin *et al.* 2010). It was observed that 10-mm aggregate and quarry dust could meet the standards even with complete aggregate replacement and increase the water absorption ratio (Ephraim and E.O 2015). Previous studies (Tammam *et al.* 2021, Ziada *et al*. 2021) were used industrial wastes as filler materials in geopolymer mortars.
This paper studies the experimental results of sulfate attack on geopolymer mortar based on fly ash (FA) using various waste materials as fine filler aggregates. The river sand (RS) was used as fine aggregate in the control series. Three different quarry dust wastes, limestone (LS), marble waste (MS), and basalt waste (BS), were used instead of the fine aggregate of river sand in the different ratios of 25%, 50%, 75% to produce ten series of geopolymer. The effects of sulfate exposure of 10% sodium sulfate (Na_2SO_4) and 10% magnesium sulfate ($MgSO_4$) up to 12 months on the prepared geopolymer specimens were studied. The mechanical properties, weight change, and ultrasonic pulse velocity (UPV) were tested for different periods, such as 2, 4, 6, and 12 months, compared with 28 days values. Moreover, the microstructural properties and polymerization reactions were studied by scanning electron microscopy (SEM) and EDS after 12 months of immersion in sulfate. In addition, the prepared samples were tested for the freeze-thaw effect of 180 cycles.

Furthermore, waste materials have a wide range of environmental and economic benefits. This research aims to utilize the unused waste quarry dust (LS, MS, BS), providing an economical and environmentally friendly geopolymer. The friendly geopolymer could reduce industrial waste disposal, minimize energy-intensive building materials, and create significant cost savings in production. However, there is limited research on using waste materials as fillers in fly ash-based geopolymers that meet conventional standards. The mechanical properties, durability properties, and microstructure analyses were investigated in this research.

Table 1 Chemical composition of (FA) and (GGBS)

Oxides	SiO_2	Al_2O_3	Fe_2O_3	CaO	MgO	SO_3	Na_2O	free CaO	Cl -	LOI
FA % by weight	54.08	26.08	6.681	2.002	2.676	0.735	0.79	0.11	0.092	1.36
GGBS % by weight	40.55	12.83	1.10	35.58	5.87	0.18	0.79	----	0.0143	0.03

Table 2 Chemical properties of sodium hydroxide (%)

NaOH (g/kg)	Na_2CO_3 (g/kg)	SO_4	Fe	Cl	Al
≥990	≤4	≤0,01	≤0.002	≤0.01	≤0.002

Table 3 Chemical properties of sodium silicate (%)

Na_2O	SiO_2	Density (20°C) (g/ml)	Fe	Heavy metals value (pb)
9.68	26.12	1.367	<0.005	<0.005

Table 4 Chemical compositions and physical properties of filler materials

Materials	LS %	MS %	BS %	RS %
SiO_2	4.93	0.70	56.9	96.7
Al_2O_3	0.82	0.29	17.6	1.05
Fe_2O_3	0.58	0.12	8.1	0.56
TiO_2	_		0.9	
CaO	51.97	55.49	8.15	0.08
MgO	0.58	0.23	2.1	_
K_2O	_	1.80	1.9	0.12
Na_2O	_	2.44	3.8	0.12
SO_3	_	_	_	_
Loss of Ignition	40.40	42.83	_	0.29
P_2O_5	_		0.2	_
MnO	_		0.1	_
Specific Gravity	2.79	2.71	2.76	2.63
Blaine (cm^2/g)	2500	8888	6285	3500

2. Materials characterization

Class F fly ash with a Blaine fineness of 2571 cm^2/g and a specific gravity of 1.98 g/cm^3 was used according to ASTM C618 standards. Also, it was contained the principal oxides (i.e., Al_2O_3, SiO_2, and Fe_2O_3) with a ratio of 70 % in terms of oxides contents. The ground granulated blast furnace Slag (GGBS) was obtained from Bolu cement company with a Blaine fineness of 2612 cm^2/g, and a specific gravity of 2.91 g/cm^3 with a hydration modulus of 1.70 was used for the study. The chemical composition is shown in Table 1 for ground granulated blast-furnace slag and fly ash.

The alkali activator used was Sodium hydroxide (NaOH) and the liquid sodium silicate (Na_2SiO_3) with the chemical composition of Na_2O=9.68% SiO_2=26.12% by mass. Both chemicals were obtained from AS Chemicals Company (Istanbul/Turkey). Tables 2 and 3 show the chemical composition of sodium hydroxide and sodium silicate, respectively.

The river sand was used as fine aggregate with a specific gravity of 2.63, bulk density of 1691 kg/m^3, and

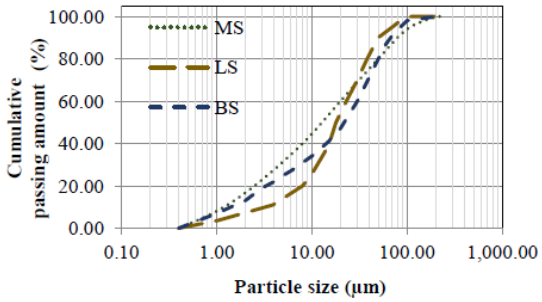

Fig. 1 The particle size distributions of LS, MS, and BS materials

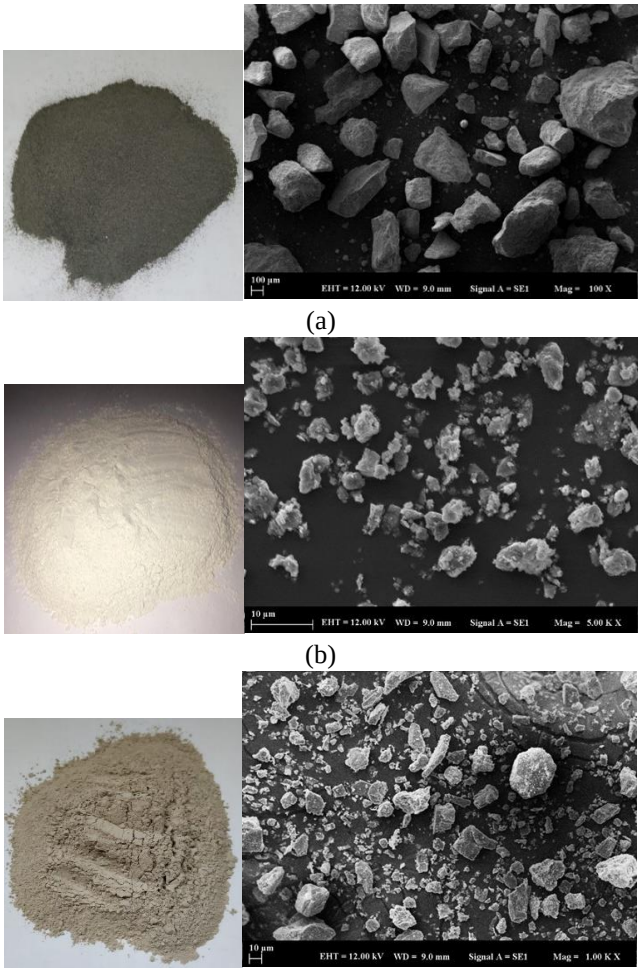

(a)

(b)

(c)

Fig. 2 The images and SEM micrographs of (a) BS, (b) MS, and (c) LS

fineness modulus of 2.8. Limestone waste powder LS was obtained from Gebze Rock Quarry/Turkey. Also, marble stone waste powder MS was obtained from Alibeykoy/Istanbul. Basalt stone powder BS was provided by INCI Group Company Sakarya/Turkey. The fillers' chemical oxides and physical properties are presented in Table 4 as analyzed by X-ray fluorescence XRF. The particle-size distributions for the LS, MS, and BS are illustrated in Fig 1. The images and SEM micrographs of the fine raw materials (powders) used in this study are shown in Fig. 2.

Table 5 Mixing quantities of geopolymer series (kg/m³)

Mix ID	GGBS	Fly ash	NaOH	Na_2SiO_3	Filler waste material	Sand
Control	69	530	132	265	0	1060
25 LS	69	530	132	265	264.93	810
50 LS	69	530	132	265	529.87	560.27
75 LS	69	530	132	265	794.8	310.54
25 MS	69	530	132	265	264.93	802.63
50 MS	69	530	132	265	529.87	545.52
75 MS	69	530	132	265	794.8	288.41
25 BS	69	530	132	265	264.93	807.3
50 BS	69	530	132	265	529.87	554.83
75 BS	69	530	132	265	794.8	302.38

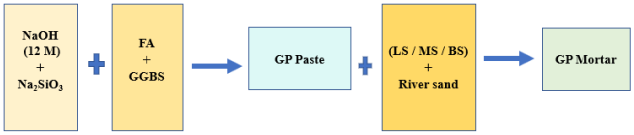

Fig. 3 Mixture procedure

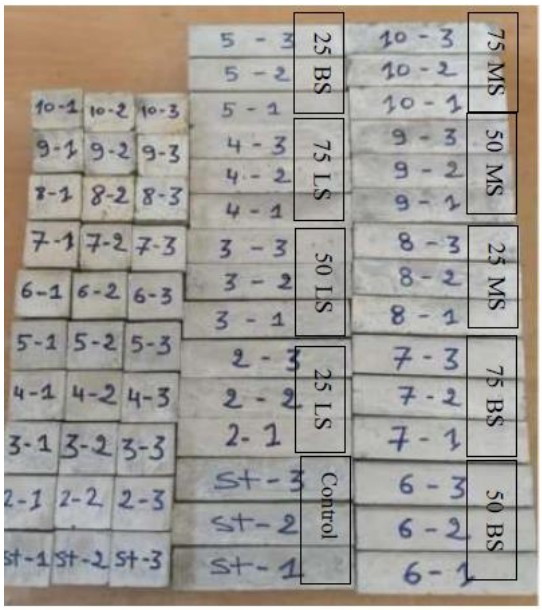

Fig. 4 Geopolymer samples before exposure to sulfate solutions

3. Experimental work

This experimental study produced ten series of geopolymer mortars with FA as a binder material and a fixed amount of about (13%) from (GGBS). Binder material FA activated in alkali silicate solution as a combination of NaOH and Na_2SiO_3; after the mixture becomes homogeneous, then adding the slag to the mix. The sodium hydroxide solution is prepared by adding one liter of distilled water to 480 g of sodium hydroxide pellets 12M (molar) and stored at room temperature for at least 24 hours before use. One-third of the activator mixture was sodium hydroxide, and two-thirds of the activator mixture was sodium silicate; the weight ratio of the binder FA to the aggregates was constant at 1:2.

The activator to binder ratio for this mixture was taken at 0.75:1. Next, the required aggregate amount was mixed in prepared fly ash paste, as shown in Fig. 3. The obtained mixture was then cast into molds to avoid the entrapped air and voids from the sample molds on the vibrator. After an hour of casting heat, curing was applied to all the specimens at 80 C° for 24 hours using an oven; the samples were kept in laboratory conditions until the scheduled tests. The mixtures ratios for the synthesized series are shown in Table 5. Previous trial mixes and literature reviews were used to prepare the mixture (Görhan *et al.* 2016, Tammam *et al.* 2021, Zamanabadi *et al.* 2019). Following the mixing procedure, 50 mm cube specimens were cast for the compressive strength test, 40 mm×40 mm×160 mm prisms for the flexural strength test, as Fig. 4 shows.

A compressive strength test was obtained after 28 days, based on ASTM C 109. According to ASTM C, 348 flexural strength test was applied after 28 days. An ultrasonic pulse velocity (UPV) test was carried out 28 days before the flexural testing on prismatic specimens to check the quality of manufactured geopolymer specimens. The resistance of manufactured geopolymer samples under 10% Na_2SO_4 or $MgSO_4$ solutions was investigated for up to 360 days. The strength properties results were obtained at 28 days for residual strength compared to the test values at 60, 120, 180, and 360 days. The solution volume was not less than five times the samples' volume cured and preserved during the test. Every 60 days, the sulfate solutions were replaced until the 360 days completion period test. The test samples were left to dry at room temperature (25±2°C) immediately after removing sulfate solutions. A wire brush was then used to clean the surfaces from the salt caused by magnesium and sodium solutions. The compressive, flexural strength, and UPV were obtained at 60,120,180, and 360 days after exposure to the sodium and magnesium sulfate solution, compared to the 28day result before the test. The SEM, EDS, and XRD investigated the samples' microstructure deterioration under the sulfate solutions attack after 360 days. The weight change results and UPV obtained at 2, 4, 6, and 12 months were compared to 28 days before the test. In addition, the geopolymer samples were subjected to 180 freeze-thaw cycles at temperatures ranging from -20 to 12°C (6 months). One cycle was determined as 12 h at -20°C and 12 h at +20°C. Strength properties, UPV, weight loss, and visual inspection were checked after freeze-thaw tests.

4. Results and discussion

4.1 Magnesium or sodium sulfate solutions attack effects

4.1.1 Visual appearance and weight changes of samples exposed to sulfate attack

The visual appearance of specimens exposed to Na_2SO_4 and $MgSO_4$ showed in Fig. 5 after 12 months of immersion in Na_2SO_4 or $MgSO_4$ solutions. The geopolymer samples have small cracks after 12 months of immersion in sulfate. In addition, no significant signs of surface erosion, cracking, or fragmentation of the specimens were observed

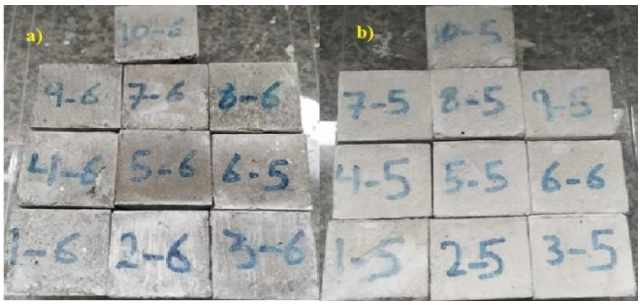

Fig. 5 The geopolymer (a) After exposure to magnesium sulfate solution12 months (b) After exposure to sodium sulfate solution12 months

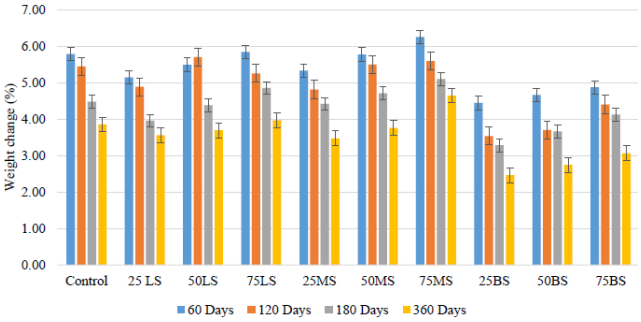

Fig. 6 Weight change after exposure with Na_2SO_4

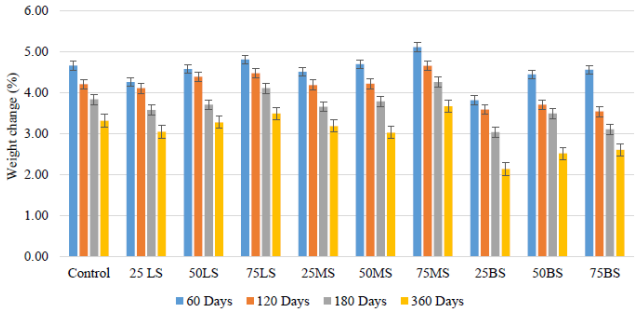

Fig. 7 Weight change after exposure with $MgSO_4$

in this study, as previous studies have shown (Aye and Oguchi 2011, Bakharev 2005, Davidovits 1989, Rajamane *et al.* 2012). After removing the specimen from the sulfate solutions and letting it dry, it was noticed that the white powdery and soft layer, besides a few needles on the surfaces of specimens, was due to prolonged immersion in sulfate solutions.

The change in weight of the manufactured geopolymer samples after exposure to 10% sodium and 10% magnesium sulfate solution was observed after 60, 120, 180, and 360 days shown in Figs. 6 and 7. In general, the weight of the samples increased slightly after immersion in the sulfate solution. As Fig. 6 shows, the control sample under the influence of sodium sulfate solution showed an increase in weight ranging between 3.85 and 5.78% up to 360 days. The weight gain for the LS category ranged from 5.14% to 5.84% after 60 days. With a range of 4.88% to 5.25% after 120 days, the weight gain percentage decreased after 360 days and ranged from 3.56% to 3.97%. The category MS showed a 5.33%-6.25% weight gain ratio at 60 days. And with a range of 4.81%-5.59% at 120 days and a range of

Table 6 Compressive strength gain/loss rates (%) due to magnesium sulfate and sodium sulfate exposure

	% Magnesium sulfate				% Sodium sulfate			
Mix ID	60 Days	120 Days	180 Days	360 Days	60 Days	120 Days	180 Days	360 Days
Control	3.28	-3.01	-6.26	-14.37	4.01	-2.69	-4.37	-10.37
25 LS	3.18	-3.27	-6.54	-15.64	3.58	-2.80	-4.70	-11.08
50LS	2.07	-3.69	-7.55	-16.46	2.51	-2.92	-5.49	-12.84
75LS	1.99	-4.22	-8.09	-18.77	2.21	-3.66	-6.00	-13.71
25MS	3.17	-3.12	-6.61	-16.05	3.78	-2.65	-5.07	-11.56
50MS	3.05	-3.39	-7.03	-17.76	3.50	-2.86	-6.23	-14.76
75MS	2.03	-3.95	-8.16	-19.01	2.47	-3.09	-7.15	-15.13
25BS	3.37	-2.98	-6.19	-13.56	4.31	-2.35	-3.80	-8.98
50BS	3.85	-2.73	-5.83	-12.56	4.62	-2.16	-3.52	-8.31
75BS	4.04	-2.32	-5.37	-10.45	4.79	-1.93	-2.83	-7.01

3.47%-4.64% at 360 days. The category BS showed a weight gain ratio of 4.44 %-4.87 % after 60 days and with a range of 3.53 %-4.40 % after 120 days, while the weight gain ratio decreased after 360 days and was in the range of 2.46 %-3.05 %. The absorption of the solution into the structure of the samples caused the samples to gain weight.

For the $MgSO_4$ solutions, as Fig. 7 shows, the weight increases of the control sample ranged between 3.31-4.65% up to 360 days, while the weight gain after 360 days was 3.04%, 3.18%, and 2.13% for 25LS, 25MS, and 25BS, respectively. The voids and porosity of the samples were almost free of water as all samples were put at 105 °C temperature for 24 hours before exposure to sodium and magnesium sulfate solutions. As a result, the weight gain of the samples could be used to evaluate the saturation of voids and pores, and microcracks that are either empty or partially filled (Bakharev 2005, Thokchom *et al.* 2010). It was also observed that fillers up to 50% enhance the change in weight ratio. The more minor weight changes occurred in the BS mixtures in sulfate solutions because BS acts as a fine filler and the samples become more compact when using BS filler.

4.1.2 Change in the strength properties

Compressive strength of sodium and magnesium sulfates

The compressive strength properties of the manufactured samples were monitored after 60, 120, 180, and 360 days of exposure to Na_2SO_4 and $MgSO_4$ solution and compared with the results of 28 days (before exposure to sulfates). The change in compressive strength is shown in Table 6 for magnesium and sodium sulfate exposure. Figs. 8 and 9 show the compressive strength of geopolymer specimens exposed to sodium sulfate and magnesium.

A slight increase in compressive strength was observed in the samples after 60 days of exposure to sulfate solutions according to 28 days of compressive strength results. The precipitation mechanisms and dissolution of the geopolymer systems mediated by alkalis cause the early age reactions (Luukkonen *et al.* 2019, Roy *et al.* 2000, Wang and

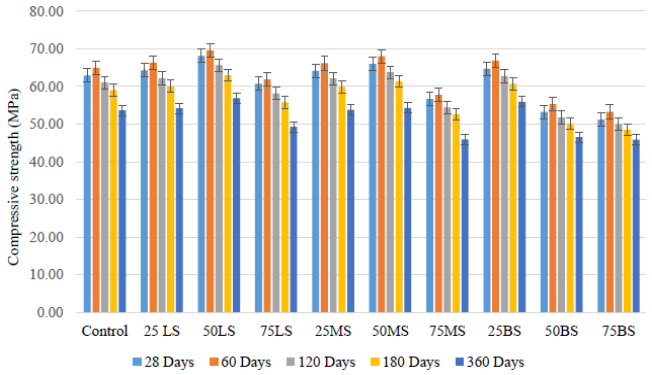

Fig. 8 Compressive strength results of geopolymer samples exposed to magnesium sulfate

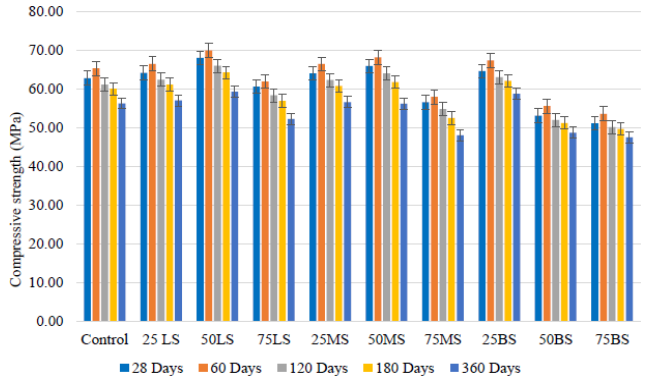

Fig. 9 Compressive strength results of geopolymer samples exposed to sodium sulfate

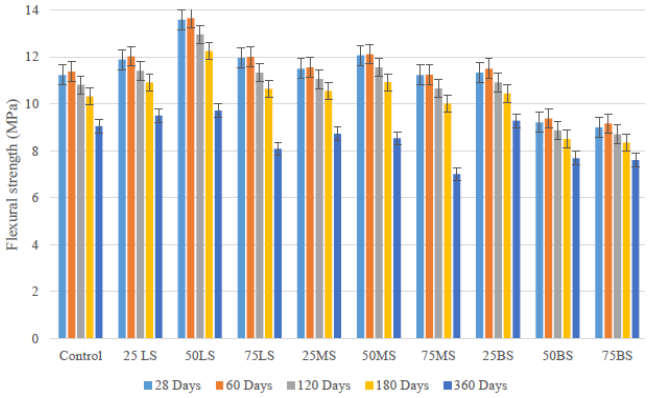

Fig. 10 Flexural strength results of geopolymer samples exposed to magnesium sulfate

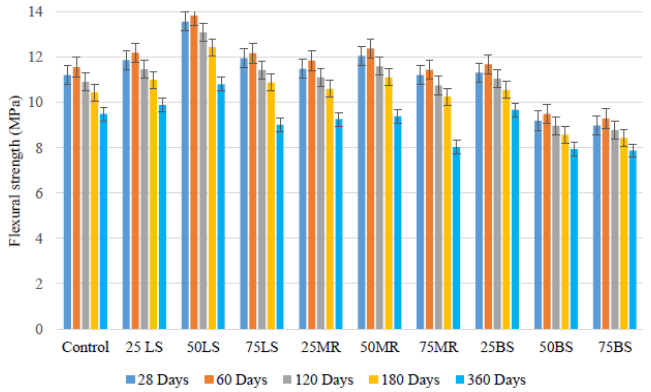

Fig. 11 Flexural strength results of geopolymer samples exposed to sodium sulfate

Scrivener 1995). The compressive strength increases up to 60 days, which confirms the high resistance and behavior of the geopolymer up to 60 days under the influence of sulfate solutions. The strength increase ranged from 2.21% to 4.79%. According to (Bakharev 2005)'s study, the increase is due to the Na ions of the sodium sulfate solution, which provide continuous hydration of the geopolymer matrix. The compressive strength of the geopolymer samples exposed to magnesium sulfate increased between 1.99% and 4.04% up to 60 days. The increase in compressive strength up to 60 days due to the continuous reaction of polymerization and pore filling by Ca dilatation products is combined with sulfate (Bakharev 2005).

After 180 days of immersion in sodium sulfate, the geopolymer specimens showed decreased strength properties; the compressive strength reduction ranged from 2.83% to 7.15% for the ten series. The drop after 180 days ranged from 5.37% to 8.16% for magnesium sulfate, higher than sodium sulfate due to its aggressive behavior. The fluctuations were observed at 120 days of exposure to magnesium sulfate due to Mg diffusion into the geopolymer matrix (Thokchom *et al.* 2010). The transition of alkalis into the solution and microcrack presence at 360 days decreased the compressive strength between 10.45% to 19.01%.

The decrease in compressive strength of the LS and MS samples was greater than that of the control and BS samples, which may be attributed to the high Ca content, which exhibits a new phase of gypsum throw Ca and the $MgSO_4$ chemical reaction that occurs during C-A-S-H' decomposition. The control and BS group samples exhibited excellent durability under the action of magnesium sulfate due to the lower Ca content and a more stable aluminosilicate polymer structure (Salami *et al.* 2017). After immersion in magnesium sulfate, the compressive strength of the control specimen was 58.95 MPa and 53.65 MPa after 180 and 360 days, respectively. The compressive strength of the 50LS sample was 62.95 MPa and 56.88 MPa, which were obtained after 180 and 360 days, respectively. The 50MS specimen had 61.35 MPa and 54.27 MPa after 180 and 360 days. 50BS had 50.10 MPa and 46.50 MPa after 180 and 360 days. The BS and control samples have shown better results under magnesium and sodium sulfate, their chemical composition, especially glass content and low Ca content. The BS powder work as a filler in the geopolymer specimens, reduces the void ratio, and diffusion of sulfate ions from the solution into the samples increases the resistance of the sulfate solutions and improves the strength properties.

Flexural strength of magnesium and sodium sulfate

The flexural strength results of the geopolymer specimens exposed to $MgSO_4$ or Na_2SO_4 solutions were obtained and compared with the 28-day results in Figs. 10 and 11. The maximum deterioration in the flexural strength of the samples was observed at the 360-day exposure time for both solutions (Thokchom *et al.* 2010). Magnesium

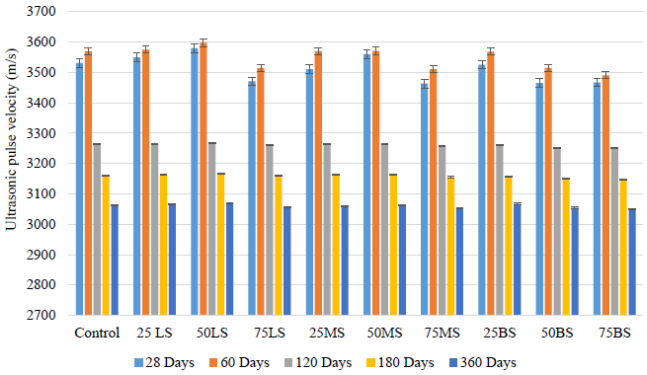

Fig. 12 UPV results of magnesium sulfate

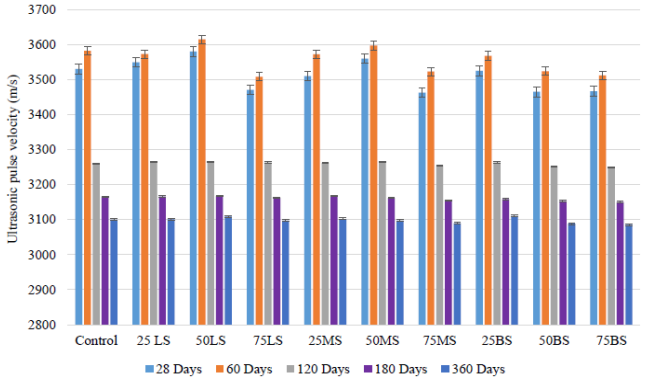

Fig. 13 UPV results of sodium sulfate

sulfate is more aggressive than sodium sulfate, which means that the flexural strength degradation is formed at the lowest sodium sulfate and magnesium sulfate (Škvára *et al.* 2005). After 60 days of $MgSO_4$ exposure, increases in flexural strength ranged from 1.17% to 3.11% for the ten mixtures. And decrease between 3.23%-5.27% after 120 days, and between 7.12%-11.04% after 180 days. After 360 days, the decrease in flexural strength ranged between 12.3%-28.4%. After 360 days of $MgSO_4$ exposure, the control sample reached a flexural strength of 9.05 MPa. Also, 50LS, 50MS, and 50BS reached 9.71 MPa, 8.73 MPa, and 7.68 MPa. After 120 days of exposure to sodium sulfate, the results of the geopolymer samples decreased between 2.22% and 4.35%. While after 180 days, the decrease was between 6.01% and 8.95%. Moreover, after 360 days, it ranged from 12.3% to 28.4%.

4.1.3 Ultrasonic pulse velocity (UPV) results

UPV results were obtained after exposure to the sulfate solutions and compared with the results after 28 days, as shown in Figs. 12 and 13. Up to 60 days, there was an increase in UPV due to the voids filled with sulfate salt (Bakharev 2005). Later, up to 120 days, the microcracks formed led to decreased results (Thokchom *et al.* 2010). Magnesium sulfate is a more aggressive solution than sodium sulfate, as seen from the UPV value (Škvára *et al.* 2005). UPV test results increase with strength after 60 days when immersed in sodium or magnesium sulfate. After 60 days, UPV increases ranged from 0.21% to 1.69% when exposed to magnesium sulfate. After 120 days, it decreased between 5.93% and 8.73%. After 180 days, it ranged from

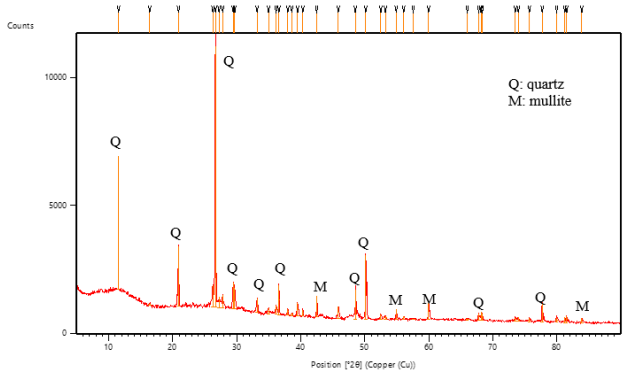

Fig. 14 X-ray diffractograms of the control sample

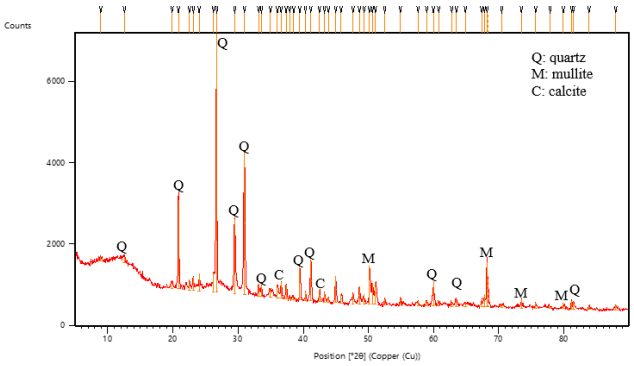

Fig. 15 X-ray diffractograms of 50% LS sample

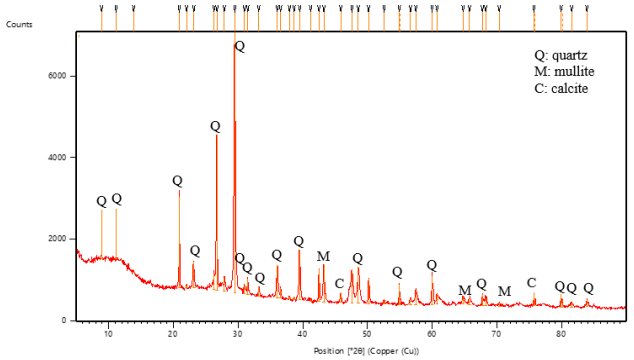

Fig. 16 X-ray diffractograms of 50% MS sample

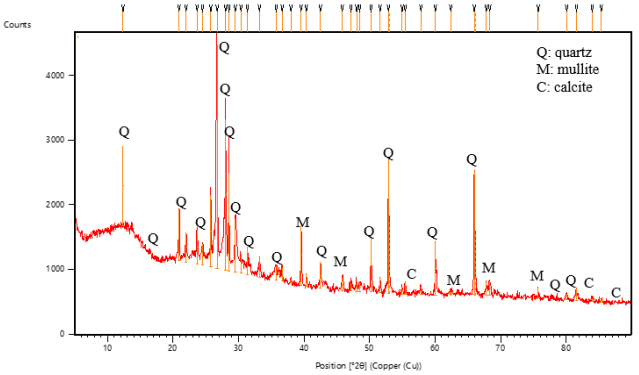

Fig. 17 X-ray diffractograms of 50% BS sample

8.8% to 11.58% under the effect of magnesium sulfate. After 360 days, the decrease under the action of magnesium sulfate was between 11.80% and 14.20%. After the

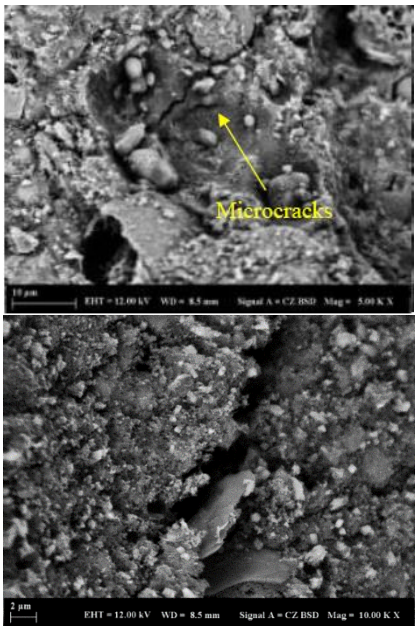

Fig. 18 The control sample after exposure to magnesium sulfate solution

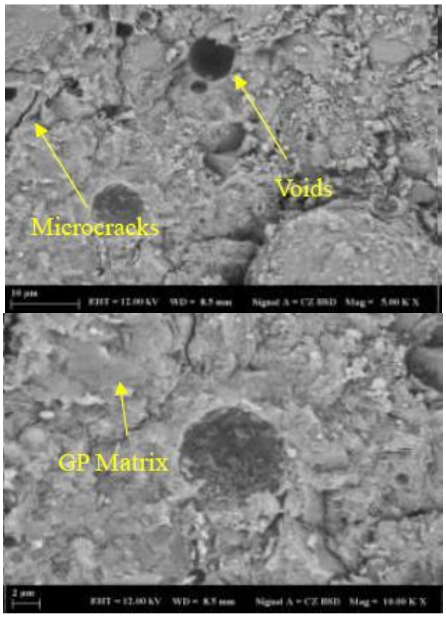

Fig. 20 The 50% MS sample after exposure to magnesium sulfate solution

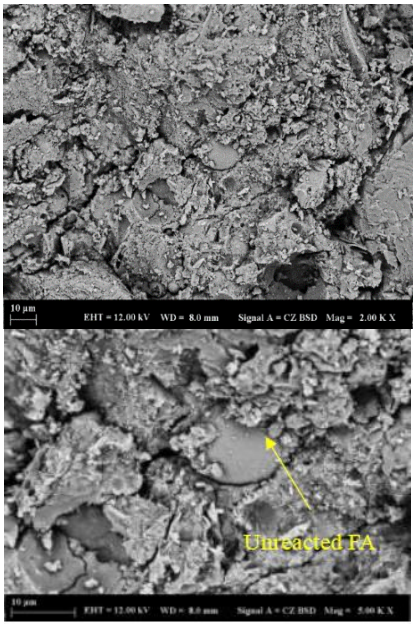

Fig. 19 The 50% LS sample after exposure to magnesium sulfate solution

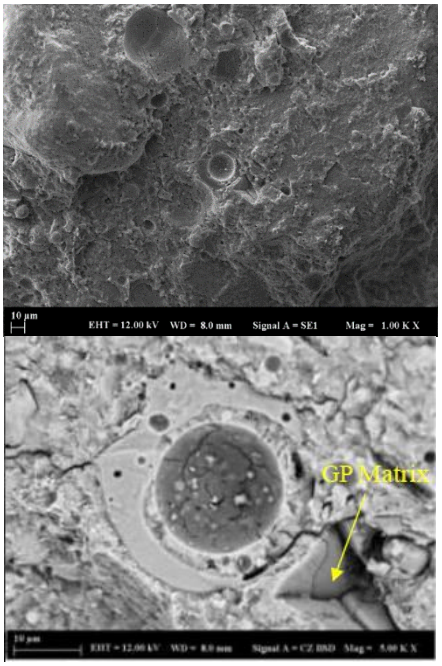

Fig. 21 The 50% BS sample after exposure to magnesium sulfate solution

samples were immersed in sodium sulfate, the increase at 60 days was between 0,67% and 1,75%. Furthermore, at 120 days, there was a decrease of between 5,97% and 8,79%; thus, after 180 days, the decrease was between 8,99% and 11,50%. after 360 days, the reduction was between 10,70% and 13%. Under the attack of magnesium sulfate, the UPV of the control sample is shown in Fig. 12. The control sample obtained 3063 m/s after 360 days. Moreover, 25LS, 50LS, 75LS were 3065 m/s, 3069 m/s and 3056 m/s, respectively. The results of 25MS, 50MS and 75MS after 360 days were 3060 m/s, 3062 m/s and 3052 m/s respectively. Also, 25BS, 50BS, 75BS were 3067 m/s, 3054 m/sand 3050 m/s respectively after 360 days.

4.1.4 The XRD analysis

The XRD analysis could be used for compound analysis. It was performed on control 50LS, 50MS, and 50BS samples. The main compounds of the geopolymerization progress are quartz, mullite, and calcite in the LS, MS, and BS specimens. Moreover, the peaks between 20-30° 2θ in all the series studied indicate satisfactory geopolymerization. Meanwhile, XRD results of control, 50LS, 50MS, and 50BS geopolymer samples are shown in Figs. 14-17. Considering the XRD results, the presence of quartz in the peaks was detected in the geopolymer samples containing various filler materials.

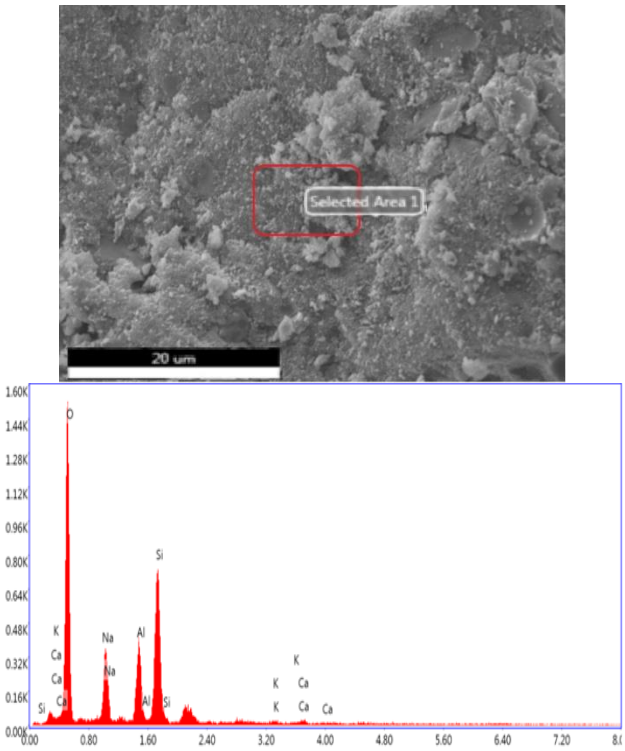

Fig. 22 EDS spectroscopy of the control sample before exposure to sulfate solution

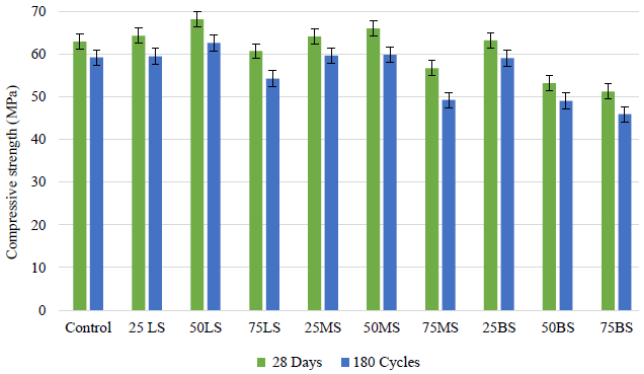

Fig. 23 Residual compressive strength results after freezing-thawing tests

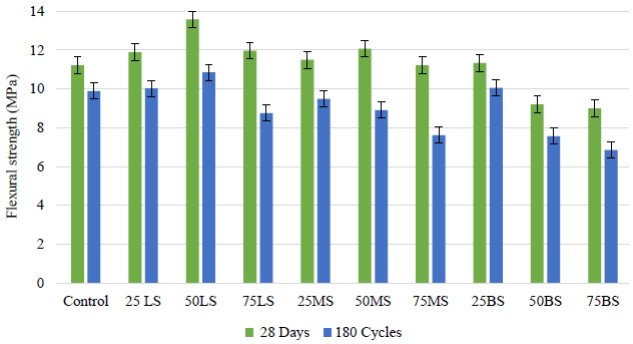

Fig. 24 Residual flexural strength results after freezing-thawing tests

This is mainly due to the high content of crystalline silica in the fly ash binder material. The most intense region where quartz peaks were observed was between 20-30° 2θ, which means that the hump is attributed to the vitreous phase of the original ash, slightly shifted from 20-30° 2θ values. In the LS, MS, and BS geopolymer series, small amounts of mullite and calcite were detected besides quartz. In the results of the marble powder-filled geopolymer mortars, low calcite peaks were observed. The different characteristic peaks may depend on the composite mixture designs, aluminosilicate source type, filler type, alkali activator type, unreacted alumina or silica, and other unreacted elements impurities. The microstructural analysis confirmed the compressive strength results of the samples.

4.1.5 Scanning electron microscope (SEM) analysis and EDS

Scanning electron microscope (SEM) testing was performed on the control, 50LS, 50MS, and 50BS samples immersed in 10% $MgSO_4$ sulfate solutions after 360 days, as shown in Figs. 18-21. In general, the SEM images of the investigated specimens reveal a sufficient degree of compactness and good microstructural bonding between the components of the geopolymeric matrix. A few unreacted fly ash particles were visible in the micrographs. The presence of unreacted FA in the geopolymer matrix particles indicates good strength behavior, as these particles positively influence the bonding pattern of the manufactured samples. Also, after 360 days of immersion with sulfate solutions, it is observed that microcracks occurred; these cracks lead to reduces in strength properties (Ferraris *et al.* 1997, Ruiz-Agudo *et al.* 2009, Santhanam *et al.* 2003). The purpose study confirms the mixes' good mechanical and durability resistance properties under the effect of magnesium sulfate.

In Fig. 22, SEM and EDS spectroscopies for the control sample before exposing sulfate could observe the matrix. Whereas Si and Al peaks represent the main products of geopolymerization, the ratio of Si/Al indicates a good microstructural bonding for manufactured samples compatible with the EDS spectroscopies. EDS can perform an elemental analysis test, indicating that O, Si, Al, Na, and Ca are present in the specimens.

4.2 Freezing-thawing test

4.2.1 Strength properties and ultrasonic pulse velocity results

After the freezing-thawing test of 180 cycles, the result was obtained and compared with the 28th-day results. The specimen's compressive and flexural strength properties are shown in Fig. 23 and 24. The specimens' dense and compact structure conducts a good degree of adhesion to the geopolymeric matrix; this led to resisting freezing-thawing and showed a good performance after 180 cycles for all categories. The volume of water increases when it freezes in the permeable structure; this is the main effect of deterioration (Pilehvar *et al.* 2019). Ice could expand in the area supplied by the air spaces in the samples. However, the freezing ice produces the cement matrix's pressure when the usable free space is filled up. Micro-cracks and disintegration occur as strength value exceeds concrete's

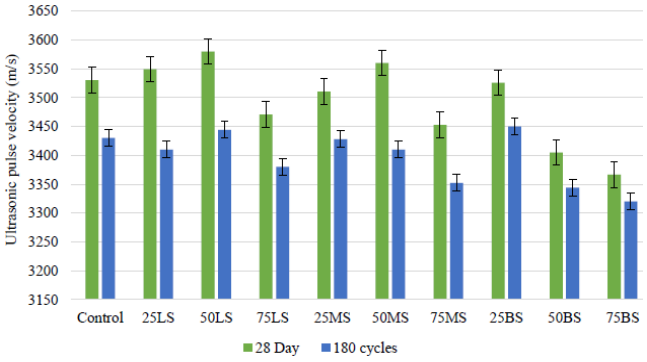

Fig. 25 UPV result after the freezing-thawing test

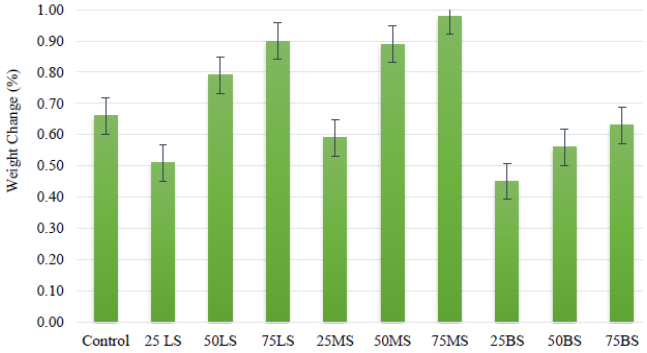

Fig. 26 Weight change (%) rate results after freezing-thawing tests

stress (Allahverdi *et al.* 2014, Basheer *et al.* 2001). The microstructural studies showed that the water changed from one state to another during the freeze-thaw cycles.

Moreover, microcracks formed in the interface between the aggregate and the paste. The microcracks may cause deterioration of the mortar, resulting in loss of strength (Sun and Wu 2013). After 180 cycles of the freezing-thawing test were implemented, the highest compressive strength value was gained with 62,55 MPa for 50 LS samples. Also, the lowest compressive strength value was 45,88 MPa for the 75BS. The same as the flexural strength, the highest value was 10,85 MPa for the 50LS, while the lowest was 6,85 MPa for 75BS.

As presented in Fig. 25, the highest and lowest results obtained after the UPV test were 3444m/s and 3320 m/s for 50LS and 75BS, respectively. The good pozzolan characteristic of fly ash and the fines structure of waste filler materials show the geopolymer samples' acceptable behavior against the freezing-thawing effect.

4.2.3 Weight change ratio

Weight loss remained below 1% in all samples (Fig. 26). The highest weight loss was in sample 75MS at 0,98%, and the lowest weight loss was in the 25BS and 25LS, respectively. The common condition observed when examining weight loss is minimal for the freeze-thaw effect. Due to the humidity of the test environment, the weight losses were minimal. The obtained result was confirmed by earlier research (Değirmenci 2018, Slavik *et al.* 2008).

5. Conclusions

- While the compressive strength of the samples exposed to sulfate increased slightly up to 60 days, the compressive strength of the samples started to decrease after 60 days. In addition, after four months, the strength values of the samples showed a decline. Sulfate solutions infiltrated the interior structure of the samples within the first two months, positively affecting the geopolymerization process. After that, minute cracks appeared in the samples, and the samples' strength began to deteriorate.
- The compressive strength loss of geopolymer samples exposed to sodium sulfate for 180 days varied between 2.83 and 7.15%. In addition, the compressive strength loss of geopolymer samples exposed to sodium sulfate for 180 days ranged from 5.37 to 8.16%. Thus, the produced geopolymer samples performed better in the Na_2SO_4 solution than in the $MgSO_4$ solution for all blends. The strength properties study reveals lower reduction values, indicating that the $MgSO_4$ attack is more aggressive than the Na_2SO_4 attack. The compressive strengths of the control, 50LS, 50 MS, and 50BS samples exposed to magnesium sulfate for 360 days were 53.65, 56.88, 54.27, and 46.52 MPa, respectively.
- The sulfate solutions' diffusion ions increase the specimen's void fraction, which reduces the resistance and strength properties. The filler addition of up to 50% reduces the pores and voids and increases the resistance of the geopolymer matrix under the sulfate attack of the specimens.
- After the sulfate exposure, there was a slight increase in the weight of the samples due to the absorption of the sulfate solution and the formation of reaction products on the exposed surface and within the pores.
- After 180 cycles of freezing-thawing, the compressive strength of 50 LS samples reached 62,55 MPa. Additionally, the 75BS had the lowest compressive strength of 45,88 MPa. As with the flexural strength, the 50LS had the most significant value of 10,85 MPa, while the 75BS had the lowest value of 6,85 MPa. Thus, quarry waste products could be used as filler materials in geopolymer. As a result, the geopolymer matrix performed admirably in the freeze-thaw test. After 180 cycles, the strength reductions and UPV results were minimal. The compact structure of the geopolymeric composite creates a high level of adhesion.

References

Abora, K., Beleña, I., Bernal, S.A., Dunster, A., Nixon, P.A., Provis, J.L., Tagnit-Hamou, A. and Winnefeld, F. (2014), "Durability and testing-Chemical matrix degradation processes", *Alkali Activated Mater.*, 177-221. https://doi.org/10.1007/978-94-007-7672-2_8.

Allahverdi, A., Abadi, M.M.B.R., Anwar Hossain, K.M. and Lachemi, M. (2014), "Resistance of chemically-activated high phosphorous slag content cement against freeze-thaw cycles", *Cold Regions Sci. Tech.*, **103**, 107-114.

https://doi.org/10.1016/j.coldregions.2014.03.012.
Aye, T. and Oguchi, C.T. (2011), "Resistance of plain and blended cement mortars exposed to severe sulfate attacks", *Constr. Build. Mater.*, **25**(6), 2988-2996. https://doi.org/10.1016/j.conbuildmat.2010.11.106.
Bakharev, T. (2005), "Durability of geopolymer materials in sodium and magnesium sulfate solutions", *Cement Concrete Res.*, **35**(6), 1233-1246. https://doi.org/10.1016/j.cemconres.2004.09.002.
Basheer, L., Kropp, J. and Cleland, D.J. (2001), "Assessment of the durability of concrete from its permeation properties: A review", *Constr. Build. Mater.*, **15**(2), 93-103. https://doi.org/10.1016/S0950-0618(00)00058-1.
Bernal Susan, A., Mejía de Gutiérrez, R. and Provis, J.L. (2012), "Engineering and durability properties of concretes based on alkali-activated granulated blast furnace slag/metakaolin blends", *Constr. Build. Mater.*, **33**, 99-108. https://doi.org/10.1016/j.conbuildmat.2012.01.017.
Bernal, S.A, Herfort, D. and Skibsted, J. (2011), "Hybrid binders based on alkali sulfate-activated Portland clinker and metakaolin", *XIII ICCC International Congress on the Chemistry of Cement*, Madrid.
Bonen, D. and Cohen, M.D. (1992), "Magnesium sulfate attack on Portland cement paste-I. Microstructural analysis", *Cement Concrete Res.*, **22**(1), 169-180. https://doi.org/10.1016/0008-8846(92)90147-N.
Brough, A.R. and Atkinson, A. (2002), "Sodium silicate-based, alkali-activated slag mortars: Part I. Strength, hydration and microstructure", *Cement Concrete Res.*, **32**(6), 865-879. https://doi.org/10.1016/S0008-8846(02)00717-2.
Cai, L., Wang, H. and Fu, Y. (2013), "Freeze-thaw resistance of alkali-slag concrete based on response surface methodology", *Constr. Build. Mater.*, **49**, 70-76. https://doi.org/10.1016/j.conbuildmat.2013.07.045.
Celik, T. and Marar, K. (1996), "Effects of crushed stone dust on some properties of concrete", *Cement Concrete Res.*, **26**(7), 1121-1130. https://doi.org/10.1016/0008-8846(96)00078-6.
Chang, F.C., Lee, M.Y., Lo, S.L. and Lin, J.D. (2010), "Artificial aggregate made from waste stone sludge and waste silt", *J. Envir. Manag.*, **91**(11), 2289-2294. https://doi.org/10.1016/j.jenvman.2010.06.011.
Chotetanorm, C., Chindaprasirt, P., Sata, V., Rukzon, S. and Sathonsaowaphak, A. (2013), "High-calcium bottom ash geopolymer: Sorptivity, pore size, and resistance to sodium sulfate attack", *J. Mater. Civil Eng.*, **25**, 105-111. https://doi.org/10.1061/(ASCE)MT.1943-5533.0000560.
Davidovits, J. (1989), "Geopolymers and geopolymeric materials", *J. Therm. Analy. Calorimetry*, **35**(2), 429-441. https://doi.org/10.1007/BF01904446.
Değirmenci, F.N. (2018), "Freeze-Thaw and fire resistance of geopolymer mortar based on natural and waste pozzolans".
Douglas, E., Bilodeau, A., Brandstetr, J. and Malhotra, V.M. (1991), "Alkali activated ground granulated blast-furnace slag concrete: Preliminary investigation", *Cement Concrete Res.*, **21**(1), 101-108. https://doi.org/10.1016/0008-8846(91)90036-h.
Duxson, P, Mallicoat, S.W., Lukey, G.C., Kriven, W.M. and van Deventer, J.S.J. (2007), "The effect of alkali and Si/Al ratio on the development of mechanical properties of metakaolin-based geopolymers", *Colloids Surfaces A: Physicochem. Eng. Aspects*, **292**(1), 8-20. https://doi.org/10.1016/j.colsurfa.2006.05.044.
Duxson, Peter, Provis, J.L., Lukey, G.C., Mallicoat, S.W., Kriven, W.M. and van Deventer, J.S.J. (2005), "Understanding the relationship between geopolymer composition, microstructure and mechanical properties", *Colloids Surfaces A: Physicochem. Eng. Aspects*, **269**(1), 47-58. https://doi.org/10.1016/j.colsurfa.2005.06.060.
Džunuzović, N., Komljenović, M., Nikolić, V. and Ivanović, T. (2017), "External sulfate attack on alkali-activated fly ash-blast furnace slag composite", *Constr. Build. Mater.*, **157**, 737-747. https://doi.org/10.1016/j.conbuildmat.2017.09.159.
Elyamany, H.E., Abd Elmoaty, A.E.M. and Elshaboury, A.M. (2018), "Magnesium sulfate resistance of geopolymer mortar", *Constr. Build. Mater.*, **184**, 111-127. https://doi.org/10.1016/j.conbuildmat.2018.06.212.
Ephraim, M. and E.O, R.L. (2015), "Elasticity and durability of concrete made with quarry rock dust and washed 10 mm gravel as aggregates", *Am. J. Eng. Tech. Soc.*, **2**, 52-59.
Fernández-Jiménez, A., Palomo, J.G. and Puertas, F. (1999), "Alkali-activated slag mortars: Mechanical strength behaviour", *Cement Concrete Res.*, **29**(8), 1313-1321. https://doi.org/10.1016/S0008-8846(99)00154-4.
Ferraris, C.F., Clifton, J.R., Stutzman, P.E. and Garboczi, E.J. (1997), "Mechanisms of degradation of Portland cement-based systems by sulfate attack", *Mech. Chem. Degrad. Cement Based Syst.*, **1997**, 185-192.
Fu, Y., Cai, L. and Yonggen, W. (2011), "Freeze-thaw cycle test and damage mechanics models of alkali-activated slag concrete", *Constr. Build. Mater.*, **25**(7), 3144-3148. https://doi.org/10.1016/j.conbuildmat.2010.12.006.
Galetakis, M. and Raka, S. (2004), "Utilization of limestone dust for artificial stone production: An experimental approach", *Min. Eng.*, **17**, 355-357. https://doi.org/10.1016/j.mineng.2003.10.031.
Görhan, G., Aslaner, R. and Şinik, O. (2016), "The effect of curing on the properties of metakaolin and fly ash-based geopolymer paste", *Compos. B Eng.*, **97**, 329-335. https://doi.org/10.1016/j.compositesb.2016.05.019.
He, P., Wang, M., Fu, S., Jia, D., Yan, S., Yuan, J., Xu, J., Wang, P. and Zhou, Y. (2016), "Effects of Si/Al ratio on the structure and properties of metakaolin based geopolymer", *Ceram. Int.*, **42**(13), 14416-14422. https://doi.org/10.1016/j.ceramint.2016.06.033.
Hill, A.R., Dawson, A.R. and Mundy, M. (2001), "Utilisation of aggregate materials in road construction and bulk fill", *Res Conserv. Recycl.*, **32**(3), 305-320. https://doi.org/10.1016/S0921-3449(01)00067-2.
Ismail, I., Bernal, S.A., Provis, J.L., Hamdan, S. and van Deventer, J.S.J. (2013), "Microstructural changes in alkali activated fly ash/slag geopolymers with sulfate exposure", *Mater. Struct.*, **46**(3), 361-373. https://doi.org/10.1617/s11527-012-9906-2.
Joseph, B. and Mathew, G. (2012), "Influence of aggregate content on the behavior of fly ash based geopolymer concrete", *Scientia Iranica*, **19**(5), 1188-1194. https://doi.org/10.1016/j.scient.2012.07.006.
Kapgate, S. S. and Satone, S. R. (2013), "Effect of quarry dust as partial replacement of sand in concrete", *Ind. Streams Res. J.*, **3**(5), 1-8.
Krivenko, P. V (1999), "Alkaline cements: structure, properties, aspects of durability", *Proceedings of the Second International Conference on Alkaline Cements and Concretes*, Kiev, Oranta, 3-43.
Luukkonen, T., Abdollahnejad, Z., Yliniemi, J., Mastali, M., Kinnunen, P. and Illikainen, M. (2019), "Alkali-activated soapstone waste-Mechanical properties, durability, and economic prospects", *Sustain. Mater. Tech.*, **22**, e00118. https://doi.org/10.1016/j.susmat.2019.e00118.
Madlool, N.A., Saidur, R., Hossain, M.S. and Rahim, N.A. (2011), "A critical review on energy use and savings in the cement industries", *Renew. Sustain. Ener. Rev.*, **15**(4), 2042-2060. https://doi.org/10.1016/j.rser.2011.01.005.
Maslehuddin, M., Al-Mehthel, M., Alidi, S.H., Shameem, M. and Ibrahim, M. (2010), "Effect of dust in coarse aggregates on reinforcement corrosion in concrete", *Constr. Build. Mater.*, **24**(3), 326-331. https://doi.org/10.1016/j.conbuildmat.2009.08.030.
Neupane, K., Chalmers, D. and Kidd, P. (2018), "High-strength geopolymer concrete-properties, advantages and challenges",

Adv. Mater., **7**(2), 15-25. https://doi.org/10.11648/j.am.20180702.11.

Pacheco-Torgal, F., Abdollahnejad, Z., Camões, A.F., Jamshidi, M. and Ding, Y. (2012), "Durability of alkali-activated binders: A clear advantage over Portland cement or an unproven issue?", *Constr. Build. Mater.*, **30**, 400-405. https://doi.org/10.1016/j.conbuildmat.2011.12.017.

Pilehvar, S., Szczotok, A.M., Rodríguez, J.F., Valentini, L., Lanzón, M., Pamies, R. and Kjøniksen, A.L. (2019), "Effect of freeze-thaw cycles on the mechanical behavior of geopolymer concrete and Portland cement concrete containing micro-encapsulated phase change materials", *Constr. Build. Mater.*, **200**, 94-103. https://doi.org/10.1016/j.conbuildmat.2018.12.057.

Puertas, F. and Fernández-Jiménez, A. (2003), "Mineralogical and microstructural characterisation of alkali-activated fly ash/slag pastes", *Cement Concrete Compos.*, **25**(3), 287-292. https://doi.org/10.1016/S0958-9465(02)00059-8.

Puertas, F., Mejia, R., Fernández-Jiménez, A., Delvasto, S. and Maldonado, J. (2002), "Alkaline cement mortars. Chemical resistance to sulfate and seawater attack", *Materiales de Construccion*, **52**(267), 55-71. https://doi.org/10.3989/mc.2002.v52.i267.326.

Rajamane, N.P., Nataraja, M.C., Dattatreya, J.K., Lakshmanan, N. and Sabitha, D. (2012), "Sulphate resistance and eco-friendliness of geopolymer concretes", *Ind. Concrete J.*, **86**(1), 13.

Roy, D.M., Jiang, W. and Silsbee, M.R. (2000), "Chloride diffusion in ordinary, blended, and alkali-activated cement pastes and its relation to other properties", *Cement Concrete Res.*, **30**(12), 1879-1884. https://doi.org/10.1016/S0008-8846(00)00406-3.

Ruiz-Agudo, E., Putnis, C.V, Jiménez-López, C. and Rodriguez-Navarro, C. (2009), "An atomic force microscopy study of calcite dissolution in saline solutions: The role of magnesium ions", *Geochimica et Cosmochimica Acta*, **73**(11), 3201-3217. https://doi.org/10.1016/j.gca.2009.03.016.

Sagoe-Crentsil, K., Brown, T. and Taylor, A. (2013), "Drying shrinkage and creep performance of geopolymer concrete", *J. Sustain. Cement-Based Mater.*, **2**(1), 35-42. https://doi.org/10.1080/21650373.2013.764963.

Sahu, A., Kumar, S. and Sachan, A.K. (2003), Crushed stone waste as fine aggregate for concrete", *Ind. Concrete J.*, **77**, 845-848.

Salami, B.A., Megat Johari, M.A., Ahmad, Z.A. and Maslehuddin, M. (2017), "Durability performance of Palm Oil Fuel Ash-based Engineered Alkaline-activated Cementitious Composite (POFA-EACC) mortar in sulfate environment", *Constr. Build. Mater.*, **131**, 229-244. https://doi.org/10.1016/j.conbuildmat.2016.11.048.

Santhanam, M., Cohen, M.D. and Olek, J. (2003), "Mechanism of sulfate attack: a fresh look: Part 2. Proposed mechanisms", *Cement Concrete Res.*, **33**(3), 341-346. https://doi.org/10.1016/S0008-8846(02)00958-4.

Scrivener, K.L. and Young, J.F. (1997), *Mechanisms of Chemical Degradation of Cement-Based Systems*, CRC Press.

Singh, B.G.I., Gupta, M. and Bhattacharyya, S.K. (2015), "Geopolymer concrete: A review of some recent developments", *Constr. Build. Mater.*, **85**. https://doi.org/10.1016/j.conbuildmat.2015.03.036.

Škvára, F., Jílek, T. and Kopecky, L. (2005), "Geopolymer materials based on fly ash", *Ceram. Silikaty*, **49**, 195-204.

Slavik, R., Bednarik, V., Vondruska, M. and Nemec, A. (2008), "Preparation of geopolymer from fluidized bed combustion bottom ash", *J. Mater. Proc. Tech.*, **200**(1), 265-270. https://doi.org/10.1016/j.jmatprotec.2007.09.008.

Sukmak, P., de silva, P. and Chindaprasirt, P. (2015), "Sulfate resistance of clay-portland cement and clay high-calcium fly ash geopolymer", *J. Mater. Civil Eng.*, **27**, 4014158. https://doi.org/10.1061/(ASCE)MT.1943-5533.0001112.

Sun, P. and Wu, H.C. (2013), "Chemical and freeze-thaw resistance of fly ash-based inorganic mortars", *Fuel*, **111**, 740-745. https://doi.org/10.1016/j.fuel.2013.04.070.

Tammam, Y., Uysal, M. and Canpolat, O. (2021), "Effects of alternative ecological fillers on the mechanical, durability, and microstructure of fly ash-based geopolymer mortar", *Eur. J. Envir. Civil Eng.*, 1-24. https://doi.org/10.1080/19648189.2021.1925157.

Temuujin, J., Minjigmaa, A., Davaabal, B., Bayarzul, U., Ankhtuya, A., Jadambaa, T. and MacKenzie, K.J.D. (2014), "Utilization of radioactive high-calcium Mongolian flyash for the preparation of alkali-activated geopolymers for safe use as construction materials", *Ceram. Int.*, **40**(10, Part B), 16475-16483. https://doi.org/10.1016/j.ceramint.2014.07.157.

Thokchom, S.P.G. and Ghosh, S. (2010), "Performance of fly ash based geopolymer mortars in sulphate solution", *J. Eng. Sci. Tech. Rev.*, **3**(1), 36-40. https://doi.org/10.25103/jestr.031.07.

Valencia Saavedra, W.G., Angulo, D.E. and Mejía de Gutiérrez, R. (2016), "Fly ash slag geopolymer concrete: Resistance to sodium and magnesium sulfate attack", *J. Mater. Civil Eng.*, **28**(12), 4016148.

Wang, S.D. and Scrivener, K.L. (1995), "Hydration products of alkali activated slag cement", *Cement Concrete Res.*, **25**(3), 561-571. https://doi.org/10.1016/0008-8846(95)00045-E.

Wongpa, J., Kiattikomol, K., Jaturapitakkul, C. and Chindaprasirt, P. (2010), "Compressive strength, modulus of elasticity, and water permeability of inorganic polymer concrete", *Mater. Des.*, **31**(10), 4748-4754. https://doi.org/10.1016/j.matdes.2010.05.012.

Zamanabadi, S.N., Zareei, S.A., Shoaei, P. and Ameri, F. (2019), "Ambient-cured alkali-activated slag paste incorporating micro-silica as repair material: Effects of alkali activator solution on physical and mechanical properties", *Constr. Build. Mater.*, **229**, 116911. https://doi.org/10.1016/j.conbuildmat.2019.116911.

Zhang, J., Shi, C., Zhang, Z. and Ou, Z. (2017), "Durability of alkali-activated materials in aggressive environments: A review on recent studies", *Constr. Build. Mater.*, **152**, 598-613. https://doi.org/10.1016/j.conbuildmat.2017.07.027.

Ziada, M., Erdem, S., Tammam, Y., Kara, S. and Lezcano, R.A. (2021), "The effect of basalt fiber on mechanical, microstructural, and high-temperature properties of fly ash-based and basalt powder waste-filled sustainable geopolymer mortar", *Sustain.*, **13**, 22. https://doi.org/10.3390/su132212610.

Ziada, M., Tammam, Y. and Erdem, S. (2022a), "Research of alternative ecological waste materials used in geopolymers for sustainable built environments", Urban Sustainability and Energy Management of Cities for Improved Health and Well-Being, 159-178. https://doi.org/10.4018/978-1-6684-4030-8.ch009.

Ziada, M., Tammam, Y., Erdem, S. and Lezcano, R.A. (2022b), "Investigation of the mechanical, microstructure and 3D fractal analysis of nanocalcite-modified environmentally friendly and sustainable cementitious composites", *Build.*, **12**(1), 36. https://doi.org/10.3390/buildings12010036.

CC